

A PORTABLE BIOSENSING DEVICE WITH MAGNETIC SEPARATION AND QUANTUM DOT BEAD LABELING FOR SIMPLE, RAPID, AND QUANTITATIVE DETECTION OF *SALMONELLA* TYPHIMURIUM



X. Xi, R. Wang, P. Yao, L. Yao, S. Tung, Y. Li

HIGHLIGHTS

- A portable biosensing device was designed, fabricated, and evaluated for *Salmonella* detection.
- A mixing, separation, and detection chamber (MSDC) was developed and used for *Salmonella* detection.
- The disposable MSDC prevented cross-contamination and reduced costs.
- The device was mostly automated for *Salmonella* detection and feasible for in-field applications.

ABSTRACT. Foodborne pathogenic bacteria have caused numerous illnesses and economic losses in the U.S. and the world. It is highly important for food industries to conduct in-field screening for pathogenic bacteria to ensure food safety. The objective of this study was to convert our previously developed optical biosensing method into a portable biosensing device to achieve simple, rapid, and quantitative detection of *Salmonella* Typhimurium. The device consisted of a control module, a magnetic separation module, and a fluorescence detection module. The bacteria sample, immuno-magnetic nanoparticles, and immuno-quantum dot beads were added into a mixing, separation, and detection chamber and were fully mixed in the control module. The sample was then moved to the magnetic separation module to automatically separate and concentrate the target bacteria. Finally, the fluorescence intensity was measured with the fluorescence detection module to determine the concentration of the target bacteria. The device was able to perform separation and detection of *Salmonella* with minimal manual operation with a detection limit of 5.4×10^2 CFU mL⁻¹ in 1 h. The device also showed good specificity against four selected non-target bacteria.

Keywords. Biosensing device, Fluorescence biosensor, Foodborne bacteria detection, Magnetic separation.

Foodborne illnesses cause hospitalizations, deaths, and economic losses around the globe. It is estimated that 600 million people fall ill because of contaminated food every year, with a death toll of 420,000 (WHO, 2019). In the U.S., there are around 48 million illnesses, 128,000 hospitalizations, 3,000 deaths, and more than \$15.6 billion in costs every year due to foodborne illnesses (CDC, 2018; USDA-ERS, 2014). Since traditional

detection methods are time-consuming and laborious, novel methods are urgently needed for fast, sensitive, labor-saving, and cost-effective detection of contamination; moreover, it is also crucial to convert these methods into portable devices for in-field and on-site detection (Habimana et al., 2018). The features of a device for in-field application include easy manual operation, short detection time, preservation of biological reagents, and portability (Srinivasan and Tung, 2015).

Rapid detection methods include nucleic acid-based methods, immunology-based methods, and biosensor-based methods. Nucleic acid-based methods such as polymerase chain reaction (PCR) are often limited in terms of portability, mostly because the sample preparation procedure is relatively complicated, time-consuming, and has to be done in a lab (Mandal et al., 2011; Silva et al., 2011; Suo et al., 2010; Truchado et al., 2016; Verstraete et al., 2012; Wang et al., 2013). Immunology-based methods such as enzyme-linked immunosorbent assay (ELISA) are simple, fast, and (potentially) portable, but many of them also produce false positives (Kragstrup et al., 2013) and have higher detection limits (Kumar et al., 2008; Niu et al., 2014; Xu et al., 2013). Biosensors have many successful reported examples that have achieved simple and fast detection, and they also show

Submitted for review on 10 January 2020 as manuscript number ITSC 13880; approved for publication as a Research Article by the Information Technology, Sensors, & Control Systems Community of ASABE on 16 August 2020.

The authors are **Xinge Xi**, Graduate Research Assistant, and **Ronghui Wang**, Research Scientist, Department of Biological and Agricultural Engineering, University of Arkansas, Fayetteville, Arkansas; **Ping Yao**, Assistant Professor, College of Information and Electrical Engineering, Shenyang Agricultural University, Shenyang, China; **Lan Yao**, Graduate Student, Key Laboratory of Agricultural Information Acquisition Technology, Ministry of Agriculture, China Agricultural University, Beijing, China; **Steve Tung**, Professor, Department of Mechanical Engineering, and **Yanbin Li**, Distinguished Professor, Department of Biological and Agricultural Engineering, University of Arkansas, Fayetteville, Arkansas. **Corresponding author:** Yanbin Li, 230 Engineering Hall, University of Arkansas, Fayetteville, AR 72701; phone: 479-575-2881; e-mail: yanbinli@uark.edu.

potential for use in practical applications (Luo and Alocilja, 2017; Wang et al., 2012; Yao et al., 2018). While electrochemical biosensors often have problems with cross-contamination of the electrodes and sample background noise (Arora et al., 2011), and mass-based biosensors have either low sensitivity or require multiple washing and drying steps (Law et al., 2015), optical biosensors are fast, sensitive, and have become one of the best methods suitable for the development of portable devices and in-field applications (Khan-sili et al., 2018; Ligler and Taitt, 2002), especially quantum dot-mediated immunosensors (Nguyen et al., 2020; Wang et al., 2020; Wu et al., 2016; Yin et al., 2016).

Salmonella is a major cause of foodborne illness around the world (WHO, 2020). In the U.S., *Salmonella* causes about 1.35 million illnesses, 26,500 hospitalizations, 420 deaths, and \$3.19 billion in losses (CDC, 2020; USDA-ERS, 2014). Human salmonellosis is characterized by gastrointestinal disorders. After ingestion, *Salmonella* colonize the intestine and invade mucosal cells, resulting in inflammation and elevated levels of cyclic adenosine monophosphate (cAMP), followed by electrolyte imbalance, loss of fluid, and eventually, diarrhea (Ray and Bhunia, 2014). Currently commercialized products for rapid detection of *Salmonella* represent a balance among shorter detection time, better portability, and higher sensitivity. Generally, two types of commercial products are available. One type integrates sample collection (usually by swab), incubation, selective enrichment, and result indication (usually by color change) into a portable tube. These devices can be very sensitive, but they are also time-consuming, often requiring more than 18 h. The other type is strips. Without any incubation process, strips are generally fast and simple but have a higher detection limit. For example, the Inspector (Halo Industry, Buena Park, Cal.) can acquire a qualitative result in less than 30 min with a single strip, and Reveal 2.0 for *Salmonella* (Neogen Corp., Lansing, Mich.) can acquire test results in 15 min, but

the detection limit is 10^6 CFU mL⁻¹. When an incubation process is used, the detection limit decreases dramatically, along with a large increase in detection time and a decrease in portability.

To date, many efforts have been made in developing various optical biosensing methods using magnetic separation for isolation of *Salmonella* (Brandão et al., 2015; Du et al., 2018; Suo et al., 2010), fluorescent labeling for detection of *Salmonella* (Wang et al., 2016; Yang and Li, 2006; Zhang et al., 2009), or both (Duan et al., 2012; Kim et al., 2015; Hu et al., 2019; Wang et al., 2007; Xu et al., 2015; Xue et al., 2018). However, limited research has been reported on converting these optical biosensing methods into an automated biosensing device. Therefore, the objective of this study was to transform a manual optical biosensing method into a portable biosensing device requiring minimal operation, using *Salmonella* Typhimurium as the target bacteria.

DESIGN AND FABRICATION

BIOSENSING PRINCIPLE

The entire process of *Salmonella* separation and detection was conducted in a mixing, separation, and detection chamber (MSDC), as shown in figure 1. The sample contained both target bacteria and other non-target bacteria and was automatically mixed with immuno-magnetic nanoparticles (immuno-MNPs) and immuno-quantum dot beads (immuno-QDBs) in the control module. The target bacteria were specifically captured by the immuno-MNPs and labeled by the immuno-QDBs, forming MNP-bacteria-QDB complexes. In the magnetic separation module, these complexes were attracted to one side of the MSDC by the magnetic field generated by magnets, while non-target bacteria and biomolecules in the sample solution were later pumped out of the MSDC to a waste tank. After phosphate buffered saline

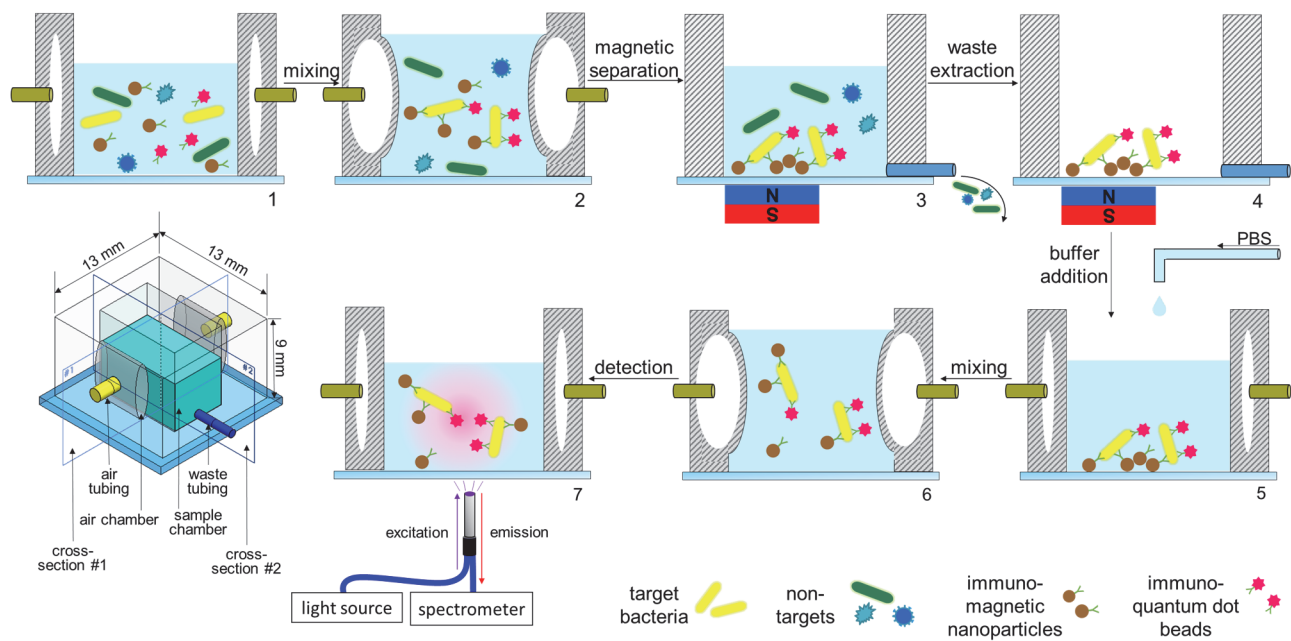


Figure 1. *Salmonella* detection process using immuno-MNPs for magnetic separation and immuno-QDBs for fluorescent labeling. A schematic of the mixing, separation, and detection chamber (MSDC) is shown in the lower left corner. Images 1, 2, 5, 6, and 7 are viewed from cross-section #1 of the MSDC schematic, and images 3 and 4 are viewed from cross-section #2.

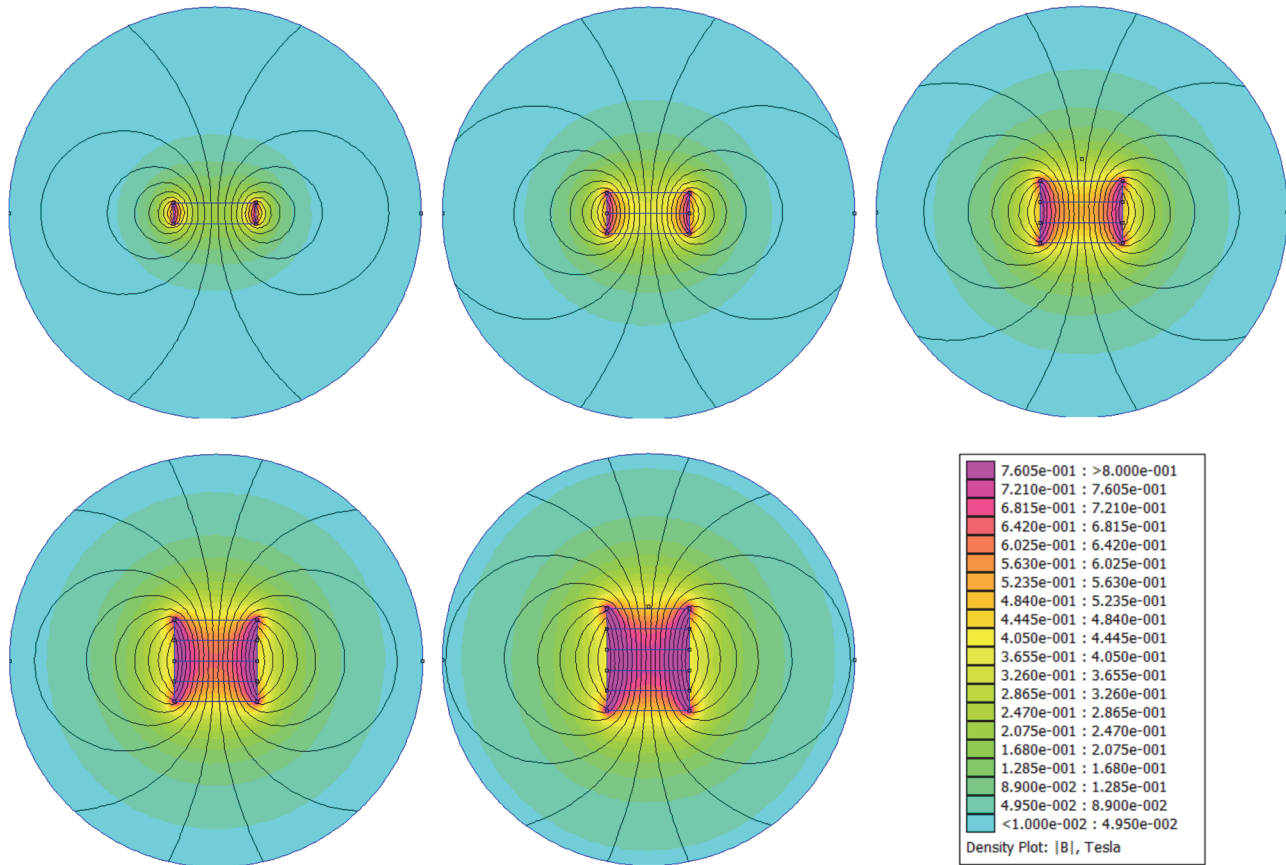


Figure 2. Simulation of magnetic field distribution with 1, 2, 3, 4, and 5 magnets.

(PBS) was added to the MSDC and mixed thoroughly to disperse the MNP-bacteria-QDB complexes evenly in the solution, fluorescence detection was conducted under the excitation of an incident light source for quantification of the target bacteria.

MAGNETIC FIELD DESIGN

To provide a magnetic field strong enough for magnetic separation, N42 magnets (B822-N42, K&J Magnetics, Pipersville, Pa.) were used to generate the magnetic field in this study. Small magnets were selected to provide flexibility in the configuration and adjustment of the magnetic field. Magnetic field simulation was done using Finite Element Method Magnetics (FEMM) software. As shown in figure 2, the magnetic field intensity increased with the number of magnets. The magnetic field reached sufficient strength when four stacked magnets were used, and more magnets did not make a noticeable difference. The magnetic field intensity was measured with a gauss meter. The maximum intensity with four stacked magnets was 4.9 kG (table 1), which was greater than that of several commercially available magnetic separators (table 2).

Table 1. Magnetic flux density with different numbers of magnets.

Number of Magnets	Maximum Magnetic Field Intensity
1	3.8 kG
2	4.5 kG
3	4.8 kG
4	4.9 kG
5	5.0 kG

PROCESS DESIGN

The device included a control module, a magnetic separation module, a PBS supply module, and a fluorescence detection module. As shown in figure 3, there were four positions for the MSDC within the device: (1) the initial position (position 1), when the sample was added to the MSDC and to which the MSDC returned when the detection process was complete; (2) the magnetic separation module (position 2), when the MSDC was moved on top of the magnets and when

Table 2. Magnetic flux density of different magnetic separators.

Separator	Maximum Magnetic Field Intensity
Dynal MPC-5	4.4 kG
PerSeptive Biosystems	2.6 kG
This study	4.9 kG

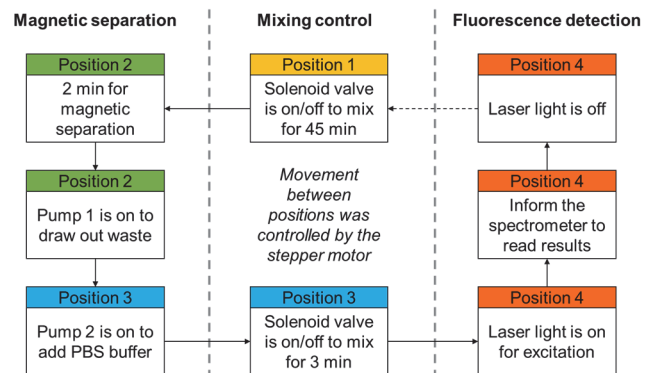


Figure 3. Components and operations of the portable biosensing device.

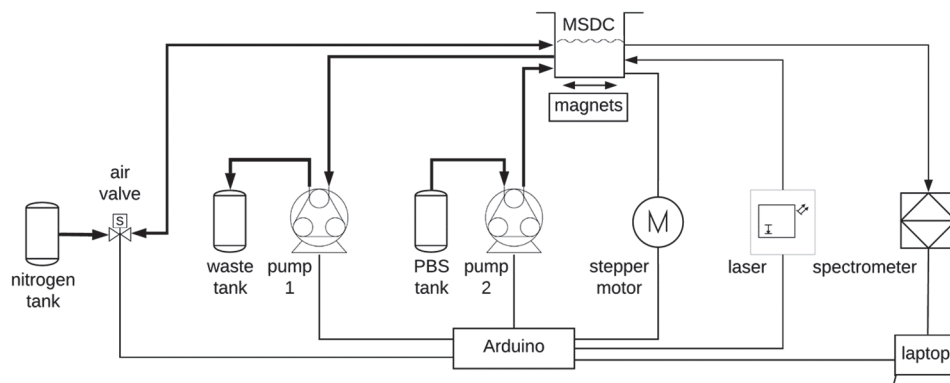


Figure 4. Process flow diagram of the portable biosensing device.

the waste pump (pump 1) extracted the waste during magnetic separation; (3) the PBS supply module (position 3), when the MSDC was placed under the PBS tubing to receive the PBS buffer droplets drawn by the PBS pump (pump 2); and (4) the fluorescence detection module (position 4), when the MSDC was moved on top of the optical fiber probe for fluorescence detection. The process flow diagram is shown in figure 4. Currently, the device can handle one sample as a batch operation. Five samples could be processed by adding more sample holders, and even more samples could be handled by increasing the size of the device.

INSTRUMENTS AND PARTS

The Arduino Uno R3 board and Adafruit Motor Shield V2 boards were products of Arduino (Somerville, Mass.). The NEMA 17 stepper motor was a product of Adafruit Industries (New York, N.Y.). The 405 nm laser was purchased from lights88-Amazon (Seattle, Wash.). The peristaltic pumps (SP101.005) were purchased from APT Instruments (Omaha, Neb.). The solenoid valve (SMC S070C-6BG-32) was purchased from Orange Coast Pneumatics (Yorba Linda, Cal.). The optical fiber (premium-grade reflection probe, VIS/NIR, UV/VIS), spectrometer (USB4000), and its driver platform (OmniDriver) were purchased from Ocean Optics (Dunedin, Fla.). The plastic protective storage case for the device was purchased from McMaster-Carr (Elmhurst, Ill.).

MIXING, SEPARATION, AND DETECTION CHAMBER (MSDC)

With modifications that included integrating a magnetic field and inserting tubing into the sample chamber for additional functions of magnetic separation and waste extraction, a disposable 3D-printed mixer previously developed by our group (Yao et al., 2019) was used for the MSDC in which all the biological reactions occurred, including fluorescence detection, as shown in figure 5. Briefly, the MSDC consisted of a sample chamber and two air chambers (fig. 1). The sample chamber was designed to contain and mix bacteria samples and reagents, while the air chambers acted as “air motors.” The air chambers were connected to a regulator installed on a nitrogen tank (Airgas, Radnor, Pa.) with the pressure set at 15 psi. The nitrogen tank was less than 36 cm in height and less than 6 kg in weight and was sufficient for supporting at least 18 h of continuous mixing. A solenoid

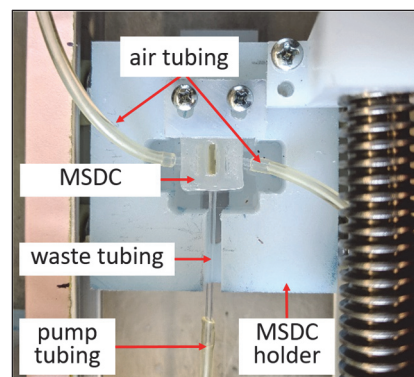


Figure 5. Photograph of MSDC and tubing connections. Air tubing was connected to the air chambers on both sides of the MSDC, and waste tubing was inserted into the sample chamber through the bottom of the MSDC, followed by pump tubing connected to the waste pump.

valve was used to control the nitrogen flow. As the valve opened, nitrogen flowed through the valve and expanded the air chambers. As the valve closed, the nitrogen in the air chambers leaked out through the exhaust port of the valve. With constant opening and closing of the valve, the nitrogen gas pushed the walls of the air chambers at a certain frequency, and the sample was mixed at the same frequency. Teflon waste tubing was inserted into the sample chamber. This tubing was connected to tubing on the waste pump. The length of the waste tubing was 15 mm to isolate the sample from the potentially contaminated tubing on the waste pump.

EXPERIMENT

CHEMICAL REAGENTS AND BIOLOGICAL MATERIALS

A Milli-Q water purification system and N-(3-dimethylaminopropyl)-N'-ethylcarbodiimide hydrochloride (EDC) were purchased from Merck KGaA (Darmstadt, Germany). The ultrapure water obtained from the Milli-Q system was used in the entire study. PBS (pH 7.4, 0.1 M) was purchased from Alfa Aesar (Haverhill, Mass.). N-hydroxysulfosuccinimide (sulfo-NHS) was purchased from Thermo Fisher Scientific (Waltham, Mass.). Bovine serum albumin (BSA) and protein A were purchased from Sigma-Aldrich (St. Louis, Mo.). Phosphate buffer (PB, pH 6.0, 0.01 M) was prepared by mixing 1.4 mM disodium hydrogen phosphate and 8.6 mM sodium dihydrogen phosphate (monohydrate), and both

were purchased from Mallinckrodt Baker (Phillipsburg, N.J.). Tryptic soy agar (TSA) was purchased from VWR (Atlanta, Ga.). Brain heart infusion (BHI) broth was purchased from Remel (Lenexa, Kan.). Purified polyclonal antibody to *Salmonella* species (4 to 5 mg mL⁻¹) and biotin conjugated polyclonal antibody to *Salmonella* species (4 to 5 mg mL⁻¹) were purchased from Meridian Life Science (Memphis, Tenn.). Magnetic nanoparticles (MNPs, 100 nm, 1 mg mL⁻¹) with streptavidin coating and quantum dot beads (QDBs, 150 nm, 10 mg mL⁻¹) with carboxylic acid groups were purchased from Ocean NanoTech (San Diego, Ca.).

CULTURES AND SURFACE PLATING METHOD

S. Typhimurium (ATCC 14028), *Listeria innocua* (ATCC 33090), *Listeria monocytogenes* (ATCC 43251), *Staphylococcus aureus* (ATCC 27660), and *Escherichia coli* O157:H7 (ATCC 43888) were obtained from the American Type Culture Collection (Rockville, Md.). Stock cultures from a -80°C freezer were grown in BHI broth at 37°C for 18 to 22 h. The live cultures were serially diluted in PBS and plated on TSA plates to determine colony numbers. The cultures were killed in boiling water for 10 min and stored at 4°C for further use.

PREPARATION OF IMMUNO-MAGNETIC NANOPARTICLES

The immuno-MNPs were prepared based on streptavidin-biotin interaction. First, 80 µL of streptavidin-coated MNPs (1 mg mL⁻¹) were washed with 60 µL of PBS, and then 40 µL of biotinylated antibodies (0.4 to 0.5 mg mL⁻¹, diluted in PBS) were added to the MNPs for conjugation of the antibodies. The mixture was incubated at 15 rpm for 45 min at room temperature, and then 50 µL of 3% BSA was added to the mixture and incubated on a rotator at 15 rpm for 30 min to block non-specific binding sites on the immuno-MNPs. The immuno-MNPs were finally washed three times with 160 µL of PBS, suspended with 160 µL of PBS, and stored at 4°C for further use. Magnetic separation was performed using a magnetic separator (MS0206, Aibit Biotech Instrument, Jiangyin, China) for 3 min.

PREPARATION OF IMMUNO-QUANTUM DOT BEADS

To prepare the immuno-QDBs, 30 µL of QDBs (10 mg mL⁻¹) were washed with 100 µL of ultrapure water, followed by centrifugation at 13,000 rpm for 5 min. After the supernatant was removed, the pellet was suspended in 200 µL of EDC/sulfo-NHS (2mM/3mM in PB) under continuous magnetic stirring at 600 rpm for 40 min. Ultrasonic homogenization of the QDBs was performed for 5 s in case of aggregation, and then 20 µL of protein A (2.5 mg mL⁻¹ in PBS) was added to the mixture and reacted with shaking at 15 rpm for 2.5 h. The excess protein A was removed after centrifugation at 13,000 rpm for 5 min, and the pellet was suspended with 200 µL of PBS, followed by incubation with 10 µL of purified antibodies (4 to 5 mg mL⁻¹), and reacted on a rotator at 15 rpm for 1 h. Finally, 100 µL of 3% BSA was added to the mixture at 15 rpm for 30 min to block non-specific binding sites. The immuno-QDBs were centrifuged at 13,000 rpm for

10 min to remove excess antibodies and BSA in the supernatant. The pellet was suspended with 120 µL of PBS at 4°C for further use.

SEPARATION AND DETECTION OF *SALMONELLA* TYPHIMURIUM

Both magnetic separation and fluorescence detection were performed using the MSDC within the portable biosensing device. After the device and the MSDC were hooked up and put into place, 50 µL of bacteria sample (or PBS as negative control), 30 µL of immuno-QDBs, and 20 µL of immuno-MNPs were added to the MSDC. After the “start” button in the software was pressed, the device began mixing the sample and moving the MSDC to four different positions to perform automatic magnetic separation, waste extraction, PBS buffer resuspension, and fluorescence detection.

In detail, after the sample and reagents were added to the MSDC at the initial position (position 1), the device mixed them for 45 min using the controlled air chambers. The MSDC was then moved by the stepper motor to the magnetic separation module (position 2) and remained there for 2 min for magnetic separation. After detectable complexes were driven by the magnet field and secured on the bottom wall inside the MSDC, pump 1 drew out the waste, and then the stepper motor moved the MSDC to the PBS supply module (position 3), where 100 µL of PBS was dropped into the MSDC by pump 2. To suspend the MNP-bacteria-QDB complexes in PBS for detection, the device performed a second mixing operation for 3 min. The stepper motor then moved the MSDC to the fluorescence detection module (position 4), where the laser provided 4.5 s of excitation at a wavelength of 405 nm. The spectrometer received the emission of QDBs at 620 nm and sent the fluorescence readings to the software that we developed. After detection, the stepper motor moved the MSDC back to position 1.

RESULTS AND DISCUSSION

HARDWARE AND SOFTWARE FOR THE PORTABLE BIOSENSING DEVICE

The portable biosensing device worked with a laptop computer, and the system setup is shown in figure 6a. Except for the optical fiber probe, all parts were mounted inside a 34 cm × 25 cm × 14 cm case (fig. 6b). Because the optical fiber probe had an 8 cm long-term bend radius (LTBR) and needed a relatively large space, it was placed outside to reduce the size of the case. Except for the fluorescence spectrometer, which was placed in the lid, all other parts were placed in the bottom of the case. The MSDC was placed in a specifically designed and fabricated holder, which included rollers on a guide rail (fig. 7), and could be moved by the stepper motor to different positions for different purposes.

Minimal operation is always preferred for in-field application, and only three steps are needed to use the device. First, the device can be quickly connected to the tubing of the nitrogen tank, the optical fiber probe connectors, the laptop, and the power supply. Second, a sample can be prepared by placing the MSDC in its holder, connecting the air tubing and waste tubing, and adding the sample and reagents to the

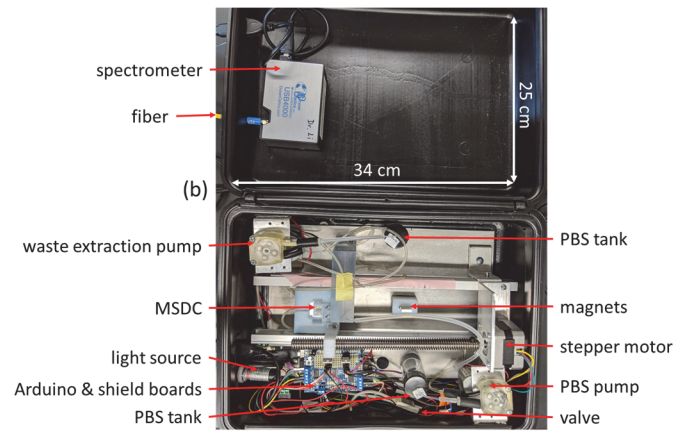
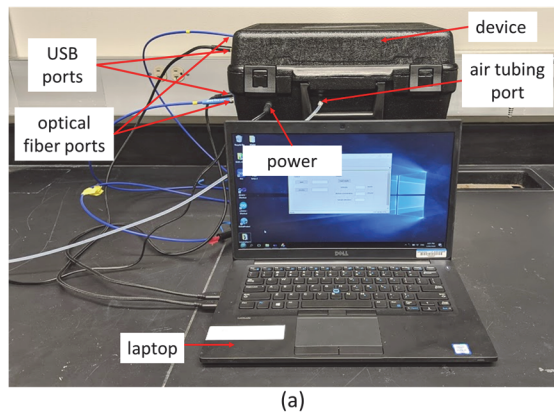


Figure 6. (a) Setup of the portable biosensing device, external connections, and laptop computer, and (b) inside layout of the device. The device sat on a frame (not shown), and the optical probe was inserted at the bottom of the device (not shown).

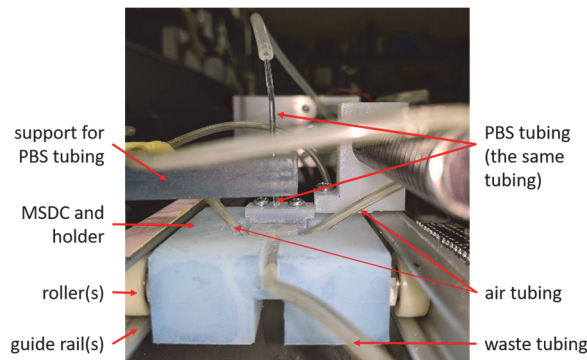


Figure 7. Photograph of MSDC at the PBS supply module. The PBS tubing was connected to the PBS pump and tank (not shown).

MSDC. Third, results can be acquired using the software’s “start” button for initiation and the “read results” button for results acquisition (fig. 8). The software displays the fluorescence intensity, the bacteria concentration calculated based on the calibration curve, and a final detection result.

EFFECTIVENESS OF MIXING AND MAGNETIC SEPARATION

A crucial problem for in-field detection of bacteria is to avoid cross-contamination among samples. In this device, cross-contamination was avoided by preventing physical interactions between the sample and the non-disposable parts of the device before the detection results were acquired. The MSDC was the sample container and was disposable; therefore, only two major actions could cause physical interactions: one was the extraction of waste from the MSDC, and the other was the addition of PBS buffer to the MSDC, both of which were closely related to the magnetic separation.

As mentioned earlier, waste was extracted by the waste pump. To avoid physical interaction between the sample and the tubing on the waste pump (which could be contaminated), extra tubing was inserted into the MSDC prior to use, which acted as a bridge to isolate the sample. In this way, before waste extraction, while the sample was still in contact with one end of the bridge tubing, the other end of the bridge tubing was clean and full of air and therefore did not pass

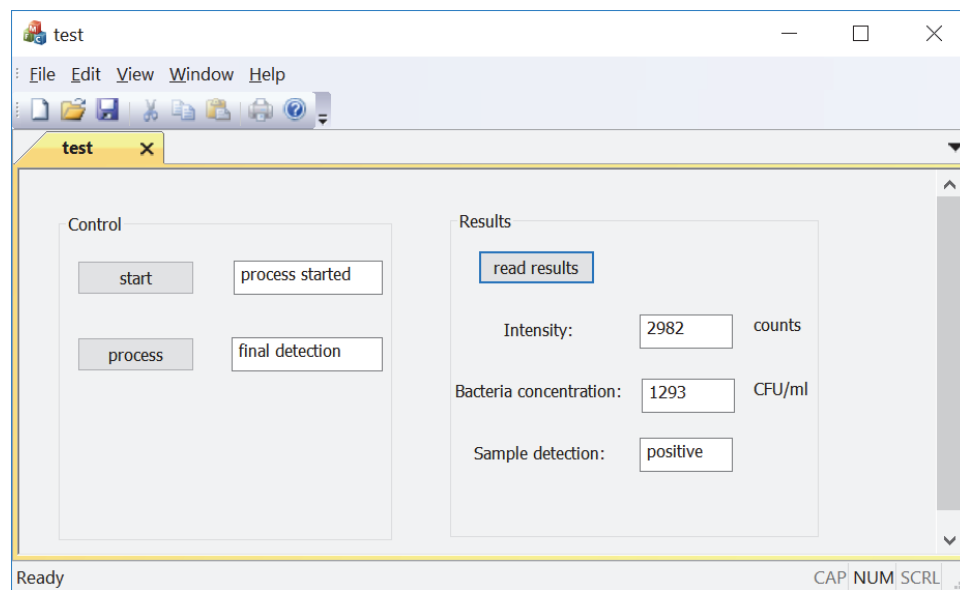


Figure 8. User interface of the developed software. In the control panel, the “start” button starts the device for sample processing and detection, and the “process” button informs the user of the current action of the device. In the results panel, the “read results” button turns on the laser, obtains readings from the spectrometer, and then moves the MSDC back to the initial position.

contamination from the waste pump tubing to the sample in the MSDC. During waste extraction, the supernatant was discarded through the waste pump tubing, and contamination from the sample entered the waste pump tubing, but not vice versa. After waste extraction, the sample was again isolated from the waste pump tubing by air.

After waste extraction, clean PBS buffer was dropped into the MSDC to suspend the MNP-bacteria-QDB complexes. (In contrast, inserting tubing into the MSDC for buffer supply could cause cross-contamination because the tubing would be full of PBS instead of air, and the sample could contaminate the PBS tubing and the PBS tank.) After the PBS buffer was dropped into the MSDC, the device automatically mixed the PBS buffer with the MNP-bacteria-QDB complexes. However, there were often some complexes caught in the corners of the MSDC, and we still needed to perform a manual step to mix the sample by pipetting. Future study on mixing, including redesign of the MSDC, optimization of the frequency, phase, and pressure used, and optimization of the speed and direction of the PBS buffer flow should be conducted to improve the mixing effect. Once this manual step of mixing is eliminated, the device will be fully automated. We also conducted fluorescence detection without PBS resuspension. Based on a test using MNP-QDB complexes, the fluorescence signal without resuspension was more than 50% higher than that with resuspension, but with a much higher variation ($\pm 36\%$ compared to $\pm 1\%$) due to the non-homogeneous distribution of the concentrated QDBs.

To confirm the effectiveness of magnetic separation, a capture efficiency test of the device was conducted. For this test, 80 μL of live *S. Typhimurium* cells and 20 μL of immuno-MNPs were added to the MSDC. After automatic magnetic separation, the sample was manually collected and plated on TSA plates, and the colonies were counted. The capture efficiency (CE) was defined as:

$$\text{CE (\%)} = \frac{N_c}{N_t} \times 100 \quad (1)$$

where N_c is the number of captured bacteria (CFU), and N_t is the number of total bacteria (CFU). The device had a capture efficiency of 96.3%, which was comparable to the capture efficiency of 99.4% when waste extraction was done manually ($n = 3$).

CALIBRATION CURVE OF THE DEVICE FOR *SALMONELLA* DETECTION

The test results for bacteria samples containing 5.4×10^1 , 10^2 , 10^3 , 10^4 , and 10^5 CFU mL^{-1} *S. Typhimurium* cells and the negative control are shown in figure 9. As the concentration of *Salmonella* increased, the fluorescence intensity increased accordingly. A linear relationship was found between the fluorescence intensity (I) and the target bacteria concentration (C): $I = 521 \times \log C + 1358$ ($R^2 = 0.99$). The calibration curve was used in the software to calculate the concentration of target bacteria based on the fluorescence measurement. The fluorescence intensity of the negative control was 2165 counts for the mean, and 207 counts for the standard deviation, and the limit of detection (LOD)

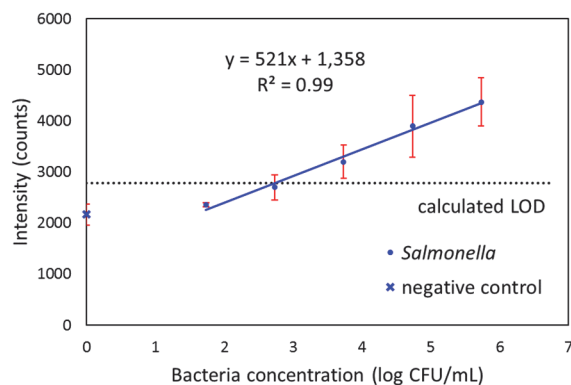


Figure 9. Linear relationship between fluorescence intensity and concentration of *S. Typhimurium* ($n = 3$). The regression equation was integrated into the software of the device for calculating the *Salmonella* concentration in CFU mL^{-1} .

calculated by summing the mean and three times the standard deviation was 2785 counts, which was equivalent to 5.4×10^2 CFU mL^{-1} ($2.73 \log$ CFU mL^{-1}). However, at the concentration of 5.4×10^2 CFU mL^{-1} , the error bar included signals less than the calculated LOD, indicating that false negative results could occur at this concentration.

The noticeable error bars could be ascribed to several causes, including lack of precision in the optical path. The position shift during the tests was performed with a simple stepper motor with open-loop control; therefore, position errors could accumulate as the test went on. Moreover, the MSDC was printed on a glass slide, and the relative position could vary because it was controlled manually during the printing process. Therefore, the optical path in each test could vary and jeopardize the precision. This can be improved by adding feedback control with a photoelectric sensor to locate the MSDC. Inaccuracy of the PBS buffer volume was a second cause of error. After magnetic separation, the MNP-bacteria-QDB complexes were suspended by the PBS buffer dropped into the MSDC through tubing. Sometimes a PBS droplet remained at the end of the tubing, causing inaccuracy in the current test and following tests. This can be improved by replacing the tubing with a pipette, which is a commercially available and market-proven tool for better liquid volume control. Valves could also be used along with the pumps for better accuracy. A third cause of error was the difference in each batch of reagents, including MNPs and QDBs. The reagents were freshly made for each test, and therefore the volume was very small, which could cause variations. The consistency should be improved when reagents are produced on a large scale and properly preserved for the tests.

SPECIFICITY OF THE DEVICE

To evaluate the specificity of the device, *L. innocua*, *L. monocytogenes*, *S. aureus*, and *E. coli* O157:H7 at a concentration of 5.4×10^4 CFU mL^{-1} were tested as non-target bacteria. In this study, specificity was ensured by the polyclonal antibodies against *Salmonella* cells. Both immuno-MNPs and immuno-QDBs were immobilized with antibodies and therefore were able to specifically capture and label the target bacteria. The fluorescence intensities of *L. innocua*, *L.*

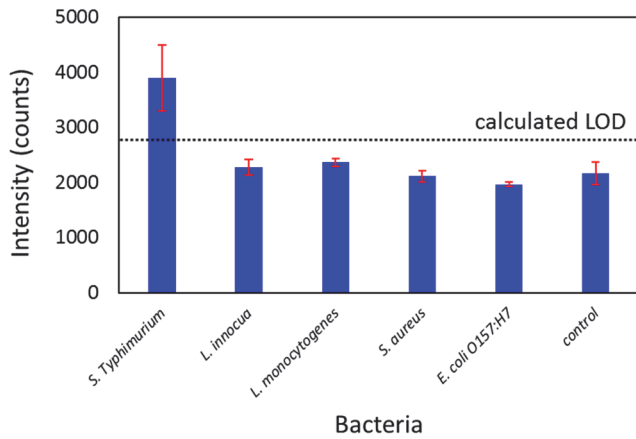


Figure 10. Specificity test of the device, where *S. Typhimurium* is the target bacteria, and *L. innocua*, *L. monocytogenes*, *S. aureus*, and *E. coli* O157:H7 are the non-target bacteria ($n = 3$). The concentration of all bacteria was 10^4 CFU mL⁻¹.

monocytogenes, *S. aureus*, *E. coli* O157:H7, and the negative control were 2276, 2366, 2114, 1967, and 2165 counts, respectively. The four non-target bacteria had signals at similar levels as the negative control, all of which were lower than the calculated LOD, as shown in figure 10. In a word, the device had good specificity in detection of *S. Typhimurium*.

Based on the similarity in signals of the non-target bacteria and the negative control, it is likely that non-target bacteria would not introduce extra noise to the device. In other words, the specificity of the bio-receptors (antibodies) used was good enough for the current device. The major concern is to reduce the relative noise level of the negative control. In addition to using more kinds of blocking reagents for the MNPs and QDBs to reduce non-specific binding, increasing the sensitivity could also be an option, including using fluorescent labels with higher emission intensities and smaller sizes. If the specificity decreases with a lower LOD, bio-receptors with higher specificity, such as monoclonal antibodies, could be considered, and more washing steps could be added.

CONCLUSIONS

In this study, we successfully developed a portable biosensing device for simple, rapid, and quantitative detection of *S. Typhimurium*. The device was able to detect *S. Typhimurium* cells in less than 1 h with a LOD of 5.4×10^2 CFU mL⁻¹. This device was mostly automated, with the limitation of an additional manual pipetting to help suspend the MNP-bacteria-QDB complexes, and has potential for in-field application of *Salmonella* detection and simultaneous detection of multiple target bacteria using their relevant antibodies and fluorescent labels with different emission wavelengths. To improve the precision and lower the LOD, future work includes improving the precision of the optical detection path and the volume of PBS buffer added. Surface modification methods could also be used to improve the sensitivity and lower the noise level.

ACKNOWLEDGEMENTS

This project was supported in part by the Walmart Foundation and Walmart Food Safety Collaboration Center. The authors thank Leland Schrader for his help with the fabrication of the device, and thank Lisa Kelso for her help in conducting microbial tests.

REFERENCES

- Arora, P., Sindhu, A., Dilbaghi, N., & Chaudhury, A. (2011). Biosensors as innovative tools for the detection of foodborne pathogens. *Biosens. Bioelectron.*, 28(1), 1-12. <https://doi.org/10.1016/j.bios.2011.06.002>
- Brandão, D., Liébana, S., Campoy, S., Alegret, S., & Isabel Pividori, M. (2015). Immunomagnetic separation of *Salmonella* with tailored magnetic micro- and nanocarriers. A comparative study. *Talanta*, 143, 198-204. <https://doi.org/10.1016/j.talanta.2015.05.035>
- CDC. (2018). Foodborne illnesses and germs. Atlanta, GA: Centers for Disease Control and Prevention. Retrieved from <https://www.cdc.gov/foodsafety/foodborne-germs.html>
- CDC. (2020). *Salmonella*. Atlanta, GA: Centers for Disease Control and Prevention. Retrieved from <https://www.cdc.gov/salmonella/index.html>
- Du, M., Li, J., Zhao, R., Yang, Y., Wang, Y., Ma, K., ... Wu, X. (2018). Effective pre-treatment technique based on immunomagnetic separation for rapid detection of trace levels of *Salmonella* in milk. *Food Control*, 91, 92-99. <https://doi.org/10.1016/j.foodcont.2018.03.032>
- Duan, N., Wu, S., Zhu, C., Ma, X., Wang, Z., Yu, Y., & Jiang, Y. (2012). Dual-color upconversion fluorescence and aptamer-functionalized magnetic nanoparticles-based bioassay for the simultaneous detection of *Salmonella* Typhimurium and *Staphylococcus aureus*. *Anal. Chim. Acta*, 723, 1-6. <https://doi.org/10.1016/j.aca.2012.02.011>
- Habimana, J. d. D., Ji, J., & Sun, X. (2018). Minireview: Trends in optical-based biosensors for point-of-care bacterial pathogen detection for food safety and clinical diagnostics. *Anal. Lett.*, 51(18), 2933-2966. <https://doi.org/10.1080/00032719.2018.1458104>
- Hu, J., Jiang, Y.-Z., Tang, M., Wu, L.-L., Xie, H.-Y., Zhang, Z.-L., & Pang, D.-W. (2019). Colorimetric-fluorescent-magnetic nanosphere-based multimodal assay platform for *Salmonella* detection. *Anal. Chem.*, 91(1), 1178-1184. <https://doi.org/10.1021/acs.analchem.8b05154>
- Khansili, N., Rattu, G., & Krishna, P. M. (2018). Label-free optical biosensors for food and biological sensor applications. *Sens. Actuators B*, 265, 35-49. <https://doi.org/10.1016/j.snb.2018.03.004>
- Kim, G., Moon, J.-H., Moh, C.-Y., & Lim, J.-G. (2015). A microfluidic nano-biosensor for the detection of pathogenic *Salmonella*. *Biosens. Bioelectron.*, 67, 243-247. <https://doi.org/10.1016/j.bios.2014.08.023>
- Kragstrup, T. W., Vorup-Jensen, T., Deleuran, B., & Hvid, M. (2013). A simple set of validation steps identifies and removes false results in a sandwich enzyme-linked immunosorbent assay caused by anti-animal IgG antibodies in plasma from arthritis patients. *SpringerPlus*, 2(1), 263. <https://doi.org/10.1186/2193-1801-2-263>
- Kumar, S., Balakrishna, K., & Batra, H. V. (2008). Enrichment-ELISA for detection of *Salmonella typhi* from food and water samples. *Biomed. Environ. Sci.*, 21(2), 137-143. [https://doi.org/10.1016/S0895-3988\(08\)60019-7](https://doi.org/10.1016/S0895-3988(08)60019-7)
- Law, J. W.-F., Ab Mutalib, N.-S., Chan, K.-G., & Lee, L.-H. (2015). Rapid methods for the detection of foodborne bacterial

- pathogens: Principles, applications, advantages, and limitations. *Front. Microbiol.*, 5(770).
<https://doi.org/10.3389/fmicb.2014.00770>
- Ligler, F. S., & Taitt, C. R. (2002). *Optical biosensors: Present and future*. Houston, TX: Gulf Professional Publishing.
- Luo, Y., & Alocilja, E. C. (2017). Portable nuclear magnetic resonance biosensor and assay for a highly sensitive and rapid detection of foodborne bacteria in complex matrices. *J. Biol. Eng.*, 11(1), 14. <https://doi.org/10.1186/s13036-017-0053-8>
- Mandal, P., Biswas, A., Choi, K., & Pal, U. (2011). Methods for rapid detection of foodborne pathogens: An overview. *American J. Food Tech.*, 6(2), 87-102.
<https://doi.org/10.3923/ajft.2011.87.102>
- Nguyen, A. V. T., Dao, T. D., Trinh, T. T. T., Choi, D.-Y., Yu, S.-T., Park, H., & Yeo, S.-J. (2020). Sensitive detection of influenza A virus based on a CdSe/CdS/ZnS quantum dot-linked rapid fluorescent immunochromatographic test. *Biosens. Bioelectron.*, 155, 112090.
<https://doi.org/10.1016/j.bios.2020.112090>
- Niu, K., Zheng, X., Huang, C., Xu, K., Zhi, Y., Shen, H., & Jia, N. (2014). A colloidal gold nanoparticle-based immunochromatographic test strip for rapid and convenient detection of *Staphylococcus aureus*. *J. Nanosci. Nanotech.*, 14(7), 5151-5156. <https://doi.org/10.1166/jnn.2014.8703>
- Ray, B., & Bhunia, A. (2014). *Fundamental food microbiology* (5th ed.). Boca Raton, FL: CRC Press.
<https://doi.org/10.1201/b16078>
- Silva, D. S. P., Canato, T., Magnani, M., Alves, J., Hirooka, E. Y., & de Oliveira, T. C. R. M. (2011). Multiplex PCR for the simultaneous detection of *Salmonella* spp. and *Salmonella* Enteritidis in food. *Intl. J. Food Sci. Tech.*, 46(7), 1502-1507.
<https://doi.org/10.1111/j.1365-2621.2011.02646.x>
- Srinivasan, B., & Tung, S. (2015). Development and applications of portable biosensors. *J. Lab. Autom.*, 20(4), 365-389.
<https://doi.org/10.1177/22111068215581349>
- Suo, B., He, Y., Tu, S.-I., & Shi, X. (2010). A multiplex real-time polymerase chain reaction for simultaneous detection of *Salmonella* spp., *Escherichia coli* O157, and *Listeria monocytogenes* in meat products. *Foodborne Pathog. Dis.*, 7(6), 619-628. <https://doi.org/10.1089/fpd.2009.0430>
- Truchado, P., Gil, M. I., Kostic, T., & Allende, A. (2016). Optimization and validation of a PMA qPCR method for *Escherichia coli* quantification in primary production. *Food Control*, 62, 150-156.
<https://doi.org/10.1016/j.foodcont.2015.10.014>
- USDA-ERS. (2014). Cost estimates of foodborne illnesses. Washington, DC: USDA Economic Research Service. Retrieved from <https://www.ers.usda.gov/data-products/cost-estimates-of-foodborne-illnesses/>
- Verstraete, K., Robyn, J., Del-Favero, J., De Rijk, P., Joris, M. A., Herman, L., ... De Reu, K. (2012). Evaluation of a multiplex-PCR detection in combination with an isolation method for STEC O26, O103, O111, O145, and sorbitol fermenting O157 in food. *Food Microbiol.*, 29(1), 49-55.
<https://doi.org/10.1016/j.fm.2011.08.017>
- Wang, C., Shen, W., Rong, Z., Liu, X., Gu, B., Xiao, R., & Wang, S. (2020). Layer-by-layer assembly of magnetic-core dual quantum dot-shell nanocomposites for fluorescence lateral flow detection of bacteria. *Nanoscale*, 12(2), 795-807.
<https://doi.org/10.1039/C9NR08509B>
- Wang, H., Li, Y., & Slavik, M. (2007). Rapid detection of *Listeria monocytogenes* using quantum dots and nanobeads-based optical biosensor. *J. Rapid Method Autom. Microbiol.*, 15(1), 67-76.
<https://doi.org/10.1111/j.1745-4581.2007.00075.x>
- Wang, L., Shi, L., Su, J., Ye, Y., & Zhong, Q. (2013). Detection of *Vibrio parahaemolyticus* in food samples using *in situ* loop-mediated isothermal amplification method. *Gene*, 515(2), 421-425. <https://doi.org/10.1016/j.gene.2012.12.039>
- Wang, X., Huang, Y., Wu, S., Duan, N., Xu, B., & Wang, Z. (2016). Simultaneous detection of *Staphylococcus aureus* and *Salmonella typhimurium* using multicolor time-resolved fluorescence nanoparticles as labels. *Intl. J. Food Microbiol.*, 237, 172-179. <https://doi.org/10.1016/j.ijfoodmicro.2016.08.028>
- Wang, Y., Ye, Z., & Ying, Y. (2012). New trends in impedimetric biosensors for the detection of foodborne pathogenic bacteria. *Sensors*, 12(3), 3449-3471. <https://doi.org/10.3390/s120303449>
- WHO. (2019). Food safety. Geneva, Switzerland: World Health Organization. Retrieved from <https://www.who.int/news-room/fact-sheets/detail/food-safety>
- WHO. (2020). *Salmonella*. Geneva, Switzerland: World Health Organization. Retrieved from https://www.who.int/foodsafety/areas_work/foodborne-diseases/salmonella/en/
- Wu, F., Yuan, H., Zhou, C., Mao, M., Liu, Q., Shen, H., ... Song Li, L. (2016). Multiplexed detection of influenza A virus subtype H5 and H9 via quantum dot-based immunoassay. *Biosens. Bioelectron.*, 77, 464-470.
<https://doi.org/10.1016/j.bios.2015.10.002>
- Xu, D., Wu, X., Li, B., Li, P., Ming, X., Chen, T., ... Xu, F. (2013). Rapid detection of *Campylobacter jejuni* using fluorescent microspheres as label for immunochromatographic strip test. *Food Sci. Biotech.*, 22(2), 585-591.
<https://doi.org/10.1007/s10068-013-0118-5>
- Xu, L., Tyson Callaway, Z., Wang, R., Wang, H., Slavik, M. F., Wang, A., & Li, Y. (2015). A fluorescent aptasensor coupled with nanobead-based immunomagnetic separation for simultaneous detection of four foodborne pathogenic bacteria. *Trans. ASABE*, 58(3), 891-906.
<https://doi.org/10.13031/trans.58.11089>
- Xue, L., Zheng, L., Zhang, H., Jin, X., & Lin, J. (2018). An ultrasensitive fluorescent biosensor using high-gradient magnetic separation and quantum dots for fast detection of foodborne pathogenic bacteria. *Sens. Actuators B*, 265, 318-325.
<https://doi.org/10.1016/j.snb.2018.03.014>
- Yang, L., & Li, Y. (2006). Simultaneous detection of *Escherichia coli* O157: H7 and *Salmonella typhimurium* using quantum dots as fluorescence labels. *Analyst*, 131(3), 394-401.
<https://doi.org/10.1039/B510888H>
- Yao, L., Wang, L., Huang, F., Cai, G., Xi, X., & Lin, J. (2018). A microfluidic impedance biosensor based on immunomagnetic separation and urease catalysis for continuous-flow detection of *E. coli* O157: H7. *Sens. Actuators B*, 259, 1013-1021.
<https://doi.org/10.1016/j.snb.2017.12.110>
- Yao, P., Wang, R., Xi, X., Li, Y., & Tung, S. (2019). 3D-printed pneumatic microfluidic mixer for colorimetric detection of *Listeria monocytogenes*. *Trans. ASABE*, 62(3), 841-850.
<https://doi.org/10.13031/trans.13245>
- Yin, B., Wang, Y., Dong, M., Wu, J., Ran, B., Xie, M., ... Chen, Y. (2016). One-step multiplexed detection of foodborne pathogens: Combining a quantum dot-mediated reverse assaying strategy and magnetic separation. *Biosens. Bioelectron.*, 86, 996-1002.
<https://doi.org/10.1016/j.bios.2016.07.106>
- Zhang, D., Carr, D. J., & Alocilja, E. C. (2009). Fluorescent barcode DNA assay for the detection of *Salmonella enterica* serovar Enteritidis. *Biosens. Bioelectron.*, 24(5), 1377-1381.
<https://doi.org/10.1016/j.bios.2008.07.081>